Received: 8 October 2019 | Revised: 13 January 2020 | Accepted: 10 February 2020

DOI: 10.1002/bit.27306

ARTICLE

BIOTECHNOLOGY BIOENGINEERING WILEY

Reprogramming of sugar transport pathways in *Escherichia coli* using a permeabilized SecY protein-translocation channel

Qiang Guo | Sen Mei | Chong Xie | Hao Mi | Yang Jiang | Shi-Ding Zhang | Tian-Wei Tan | Li-Hai Fan

Beijing Key Laboratory of Bioprocess, College of Life Science and Technology, Beijing University of Chemical Technology, Beijing, China

Correspondence
Li-Hai Fan, North Third Ring Road 15, Chaoyang, 100029 Beijing, China.
Email: fanlh@mail.buct.edu.cn

Funding information
National Natural Science Foundation of China, Grant/Award Numbers: 21776010, 21978014; The National Key Research and Development of China, Grant/Award Number: 2016YFA0204300; International Clean Energy Talent Program of China Scholarship Council, Grant/Award Number: 201802180008

Abstract

In the initial step of sugar metabolism, sugar-specific transporters play a decisive role in the passage of sugars through plasma membranes into cytoplasm. The SecY complex (SecYEG) in bacteria forms a membrane channel responsible for protein translocation. The present work shows that permeabilized SecY channels can be used as nonspecific sugar transporters in *Escherichia coli*. SecY with the plug domain deleted allowed the passage of glucose, fructose, mannose, xylose, and arabinose, and, with additional pore-ring mutations, facilitated lactose transport, indicating that sugar passage via permeabilized SecY was independent of sugar stereospecificity. The engineered *E. coli* showed rapid growth on a wide spectrum of monosaccharides and benefited from the elimination of transport saturation, improvement in sugar tolerance, reduction in competitive inhibition, and prevention of carbon catabolite repression, which are usually encountered with native sugar uptake systems. The SecY channel is widespread in prokaryotes, so other bacteria may also be engineered to utilize this system for sugar uptake. The SecY channel thus provides a unique sugar passageway for future development of robust cell factories for biotechnological applications.

KEYWORDS

fermentation, metabolic engineering, microbial metabolism, sugar utilization

1 | INTRODUCTION

Sugars are the major carbon and energy sources for living organisms. Thus, transport of sugars across the plasma membrane into the cytoplasm is an essential cell biochemical function that relies on numerous sugar-specific transport systems (L. Q. Chen, Cheung, Feng, Tanner, & Frommer, 2015; Cirillo, 1961; Reinhold & Kaplan, 1984). *Escherichia coli* is a gram-negative, facultatively anaerobic bacterium, which is one of the most important organisms for metabolic engineering because of its rapid growth, the hereditary information, and the well-developed genetic tools available (Pontrelli et al., 2018). Given the widespread interests in biotechnological applications, sugar uptake routes in *E. coli* have been intensively investigated (Luo, Zhang, & Wu, 2014). However, the sugar transporters with broad sugar profiles are still unavailable.

Sugar transport involves active and passive mechanisms. Active transport requires metabolic energy for passage of molecules across the plasma membrane against a concentration gradient, whereas passive transport moves molecules from a higher to lower concentrations without the need for energy input. Passive transport can also be classified as facilitated diffusion and free diffusion. Active transport and facilitated diffusion are dependent on specific molecular binding between cargo and transporter, exhibiting substrate stereospecificity, nonlinear kinetics, and competitive inhibition (Cirillo, 1961). Moreover, many sugars are taken up with concomitant phosphorylation via the phosphoenolpyruvate: carbohydrate phosphotransferase system (PTS), which may cause carbon catabolite repression (CCR) and lead to diauxic cell growth on sugar mixtures (Stülke & Hillen, 1999). In contrast, free diffusion is non-mediated

transport with a rate linear and in proportion to the difference in concentrations of the cargo. However, only small non-polar molecules such as carbon dioxide and oxygen are believed to freely diffuse through plasma membranes (Zhao et al., 2011). Although many sugars are transported passively, no sugars are known to enter the cells via free diffusion.

Protein translocation channels are structurally conserved protein-conducting systems that allow polypeptides to be transferred across or integrated into cell membranes (Mandon, Trueman, & Gilmore, 2009; Osborne, Rapoport, & Van den Berg, 2005; Rapoport, 2007). In bacteria, these channels are formed by the SecY complex (SecYEG) and located in the plasma membrane (Akimaru, Matsuyama, Tokuda, & Mizushima, 1991; Breyton, Haase, Rapoport, Kühlbrandt, & Collinson, 2002; Brundage, Hendrick, Schiebel, Driessen, & Wickner, 1990). X-ray crystallography revealed that the SecY channel has an hourglass shape with a narrow central constriction consisting of six hydrophobic amino acid residues termed the pore ring, and the exofacial side of the channel is occluded by a short α-helical segment called the plug domain (Figure 1a; Van den Berg et al., 2004). The SecY plug domain serves as a physical barrier that ensures that the channel is sealed in its resting state (W. Li et al., 2007). During translocation, the plug is displaced by the incoming polypeptide from the center of the channel to an open position (L. Li et al., 2016; Tam, Maillard, Chan, & Duong, 2005), and the pore ring forms a "gasket-like" seal around the polypeptide chain (Park & Rapoport, 2011), preventing permeation by other molecules. Interestingly, although deletion of the plug in *E. coli* leads to membrane leakage (Park & Rapoport, 2011), it only causes a relatively minor growth defect (W. Li et al., 2007; Park & Rapoport, 2011), which may be because the hydrophobic nature of the pore ring can still provide a barrier for certain molecules (Park & Rapoport, 2011). These findings prompted us to hypothesize that SecY may be permeabilized and used as a free diffusion channel for sugars, offering a new paradigm for sugar uptake and addressing problems encountered with native sugar-specific transporters.

In the present work, the SecY channel in *E. coli* was permeabilized through plug deletion and pore-ring mutation. Using these SecY mutants, the severe acute respiratory syndrome (SARS) coronavirus envelope protein (SCVE), and appropriate sugar kinases (Figure 1b), we demonstrated nonspecific transport of mono- and di-saccharides across the plasma membrane without requiring that *E. coli* possess a large number of sugar-specific transporters for survival, a desirable attribute for biotechnological applications.

2 | MATERIALS AND METHODS

2.1 | Strains, vectors, and media

E. coli Top10 (F^- *mcrA* Δ[*mrr-hsd*RMS-*mcr*BC] ϕ80 *lac*ZΔM15 Δ*lac*X74 *rec*A1 *ara*Δ139 Δ[*ara-leu*]7697 *gal*U *gal*K *rps*L[Str^R] *end*A1 *nup*G), and *E. coli* BL21 (DE3) (F^- *ompT hsdS*[r_B^- m_B^-] *gal dcm* [DE3]) were used in

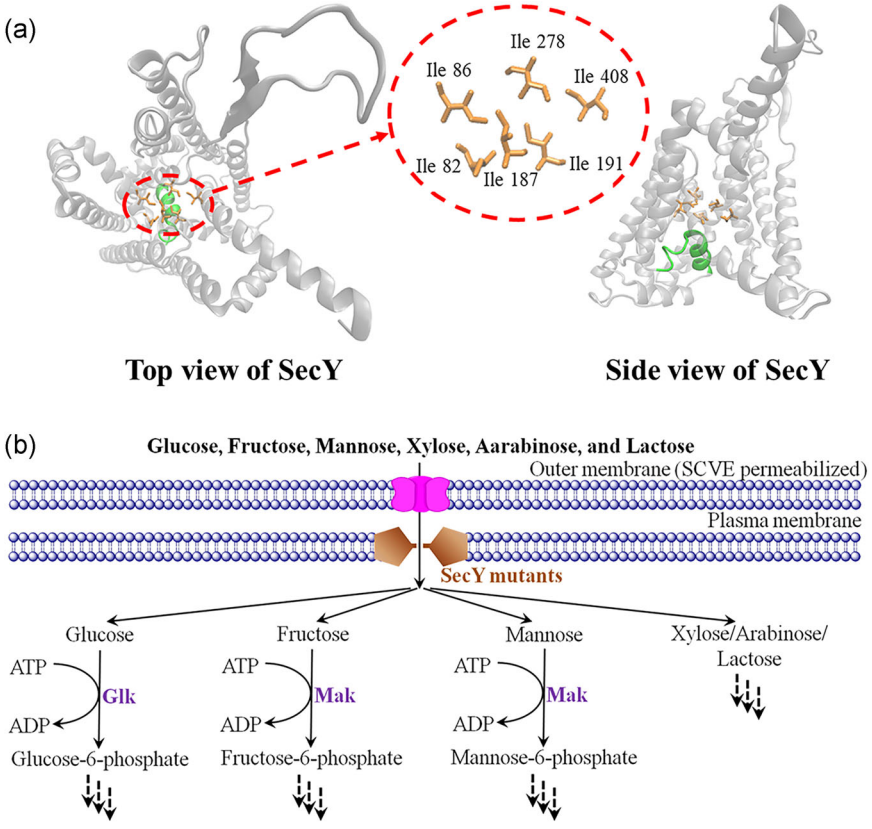

FIGURE 1 Use of SecY mutants for sugar transport in *Escherichia coli*. (a) The three-dimensional structures of the wild-type SecY channel obtained via homology modeling (VMD 1.9.2) using PDBID 3J46 as a template. The plug domain (residues 64–70) is shown in green, and the pore ring is shown in orange. Pore-ring residues of SecY: Ile 82, Ile 86, Ile 187, Ile 191, Ile 278, Ile 408. (b) Sugar uptake routes with SecY mutants. Glk, glucokinase; SCVE, SARS coronavirus envelope protein; Mak, fructo(manno)kinase [Color figure can be viewed at wileyonlinelibrary.com]

this study. *E. coli* Top10 was used for plasmid construction. The λ Red recombination system (pKD13, pKD46, and pCP20) was provided by Prof. Ping-Fang Tian (Beijing University of Chemical Technology). The plasmids pETDuet-1 (ampicillin resistance), pRSFDuet-1 (kanamycin resistance), and pACYCDuet-1 (chloramphenicol resistance) were purchased from Novagen (Merck Millipore) and used with *E. coli* BL21 (DE3) for co-expression of proteins under *T7* promoters. The Luria-Bertani (LB) cell culture medium contained 10 g/L tryptone, 5 g/L yeast extract, and 10 g/L NaCl. The M9 mineral cell culture medium (without sugars) contained 7.52 g/L $Na_2HPO_4{\cdot}2H_2O$, 3 g/L KH_2PO_4, 0.5 g/L NaCl, 0.5 g/L NH_4Cl, 0.25 g/L $MgSO_4{\cdot}7H_2O$, 44.1 mg/L $CaCl_2{\cdot}2H_2O$, 1 mg/L biotin, 1 mg/L thiamin, 50 mg/L EDTA, 8.3 mg/L $FeCl_3{\cdot}6H_2O$, 0.84 mg/L $ZnCl_2$, 0.13 mg/L $CuCl_2{\cdot}2H_2O$, 0.1 mg/L $CoCl_2{\cdot}2H_2O$, 0.1 mg/L H_3BO_3, and 0.016 mg/L $MnCl_2{\cdot}4H_2O$.

2.2 | Gene knockout

Markerless inactivation of *ptsG* (GenBank ACT42992.1), *fruA* (GenBank ACT43919.1), *manXYZ* (GenBank ACT43641.1, ACT43642.1, ACT43643.2), *xylFGH* (GenBank ACT45218.1, CP001509.3, ACT45219.1), *araFGH* (GenBank ACT43723.1, ACT43722.1, ACT43721.2), *araE* (GenBank ACT44505.1), and *lacY* (GenBank ACT42196.1) in *E. coli* BL21 (DE3) was performed using the λ Red recombination system (Datsenko & Wanner, 2000). In brief, PCR products were generated using primers (Table S1) with sequences homologous to those of regions adjacent to the gene to be inactivated and template pKD13 carrying a kanamycin resistance gene that is flanked by FLP recognition target sites. *E. coli* BL21 (DE3) harboring pKD46 was grown in LB containing 100 μg/ml ampicillin and 4 g/L arabinose at 37°C for 1 hr. After that, PCR products were transformed (MicroPulser, Bio-Rad) into cells to disrupt the chromosomal gene on LB agar plates containing 50 μg/ml kanamycin at 37°C. The kanamycin resistance gene in the gene-knockout mutant was eliminated using pCP20, which encodes the FLP recombinase at 30°C and is lost at 42°C.

2.3 | Cloning, mutation, and plasmid construction

sCVE (GenBank AAP73416.1) was codon optimized and synthesized by Inovogen Tech. Co. (Beijing, China). The sequence is listed below (5′ → 3′):

ATGTACTCGTTCGTATCTGAAGAAACCGGTACTCTGATCGTG
AATTCCGTGCTGCTGTTCCTGGCGTTCGTAGTCTTCCTGCTGGTC
ACTCTGGCTATTCTGACCGCGCTGCGTCTGTGCGCATACTGTTGT
AACATCGTAAACGTTTCCCTGGTTAAACCGACGGTATACGTATAC
TCTCGCGTCAAAAACCTGAACAGCTCCGAAGGTGTCCCGGxACC
TGCTGGTT

secY (GenBank ACT44955) was cloned via PCR from *E. coli* BL21 (DE3) using primers of *secY*-F and *secY*-R. Residues 60-74 of SecY were replaced with a short linker (GlySerGlySer) by overlap PCR, resulting in SecY (ΔP). In brief, by use of *secY* as a template, a 199-bp DNA fragment was amplified via primers of *secY1*-F and *secY1*-R, and a 1133-bp fragment was amplified by using *secY2*-F and *secY2*-R. These two fragments were then mixed and used as templates to obtain the full length gene for secY (ΔP) using *secY1*-F and *secY2*-R. SecY (ΔP, IIIGII) was obtained by changing Ile 191 into Gly based on SecY (ΔP). This mutation was also carried out by overlap PCR. The primers used were *secY1*-F, *secY2*-R, *Ring-191*-F, *Ring-191*-R. Then, the Ile 408 of SecY (ΔP, IIIGII) was replaced with Gly by use of *secY1*-F, *secY2*-R, *Ring-408*-F, *Ring-408*-R, resulting in SecY (ΔP, IIIGIG).

Protein expression in this study was carried out by use of plasmids. All genes, recombinant plasmids, recombinant strains, and other primers used are summarized in Tables S2–S5.

2.4 | Sodium dodecyl sulfate polyacrylamide gel electrophoresis (SDS-PAGE) analysis

The *E. coli* cells with appropriate plasmids were grown in 100 ml of LB medium containing 100 μg/ml ampicillin and 50 μg/ml kanamycin at 37°C and 200 rpm. After 3 hr, the protein expression was induced by addition of 0.4 mM isopropyl-β-D-thiogalactoside (IPTG) at 16°C for 12 hr. The cells were then harvested by centrifugation at 6,000*g*. They were re-suspended in phosphate buffered saline (PBS) buffer (pH 7.4) and disrupted by sonication on ice. Cellular debris was removed by centrifugation at 6,000*g* for 10 min. The His-tagged SCVE in supernatant was purified using HisTrap FF crude Column (GE). The analysis was carried out on 12% SDS-PAGE gel.

2.5 | [^{14}C]-labeled glucose transport assay

[^{14}C]-labeled glucose (5.5 mCi/mmol) was purchased from American Radiolabeled Chemicals, Inc. *E. coli* strains were induced with 0.4 mM IPTG at 25°C for 12 hr in LB supplemented with 100 μg/ml ampicillin and 50 μg/ml kanamycin. The cells were harvested by centrifugation at 5,000*g* and washed twice with PBS. After that, the strains were re-suspended in the same buffer at an $A_{600\,nm}$ of 1 (EU-2600 UV-visible spectrophotometer, Onlab, China). The reaction was initiated by adding 60 μl of [^{14}C]-labeled glucose (1 mM) to 540 μl of cell suspension at room temperature. The suspension was sampled at 5 min and centrifuged at 5,000*g* to remove the cells. Then, 500 μl of supernatant was mixed with 5 ml of scintillation cocktail. Radioactivity was measured using a Hidex 300 SL liquid scintillation counter (Hidex, Finland).

2.6 | Analysis of promoter P_{BAD} activation

The expression kinetics of green fluorescent protein (GFP) controlled by a P_{BAD} promoter on arabinose were analyzed. In brief, *E. coli* strains with the GFP expression cassette were precultured in LB containing 100 μg/ml ampicillin, 50 μg/ml kanamycin, and 30 μg/ml

chloramphenicol at 37°C overnight. The cells were then sub-inoculated into M9 medium supplemented with the same antibiotics, 0.4 mM IPTG, and 4 g/L arabinose. After growth at 37°C, the cells were harvested by centrifugation at 5,000*g* at different times and then washed twice with PBS. They were then re-suspended in PBS, and their fluorescence intensity was measured by using FACSAria II (Becton Dickinson).

2.7 | 2-Deoxy-2-([7-nitro-2,1,3-benzoxadiazol-4-yl]amino)-D-glucose (2-NBDG) transport assay

2-NBDG was purchased from Sigma-Aldrich Co. *E. coli* strains were inoculated in Luria-Bertani (LB) medium containing 100 μg/ml ampicillin and 50 μg/ml kanamycin, and then induced with 0.4 mM IPTG at 25°C for 12 hr. After harvest by centrifugation at 5,000*g* and two washes with PBS, the cells were re-suspended in PBS. A reaction was initiated by adding 2-NBDG to 10 μM at room temperature. The suspension samples were obtained at 5 min and centrifuged at 5,000*g* to remove the cells. The fluorescence of the supernatant was measured using a F-320 fluorescence spectrometer (Guangdong, China) at a λ_{Ex} of 475 nm and λ_{Em} of 550 nm (Yoshioka et al., 1996). The 2-NBDG uptake rate by *E. coli* (ΔPtsG) was considered as the background.

2.8 | Fermentation

E. coli strains were precultured in LB medium containing 100 μg/ml ampicillin and 50 μg/ml kanamycin at 37°C overnight, and then the cells were subinoculated into M9 medium supplemented with the same antibiotics, 0.4 mM IPTG, and sole sugar as the carbon source. In mixed-sugar fermentation, the carbon sources were glucose and xylose. The cell density ($A_{600\,nm}$) in sole-sugar fermentation was determined using a Multiskan Spectrum spectrophotometer (Thermo Fisher Scientific), while in mixed-sugar fermentation it was determined using a EU-2600 UV–visible spectrophotometer (Onlab, China). Sugars were measured by a high-performance liquid chromatography system (Dionex U300 HPLC; Dionex) equipped with an Aminex HPX-87H Column (Bio-Rad), with 5 mmol/L H_2SO_4 used as the mobile phase.

3 | RESULTS AND DISCUSSION

3.1 | Functional transport of PTS-dependent hexoses via the SecY (ΔP) channel

When we expressed SecY with the plug deleted (SecY [ΔP]) in *E. coli* (ΔPtsG) lacking the glucose PTS (P. T. Chen, Chiang, Wang, Lee, & Chao, 2011; Joung, Kurumbang, Sang, & Oh, 2011; Figure 2a), the cell growth defects were not observed (Figure 2b). In contrast, the limitation of growth on glucose caused by insufficient import of the sole carbon source was partially rescued. We reasoned that the SecY (ΔP) channel might allow glucose to diffuse through the plasma membrane due to its small V_A (≈ 0.178 m^3/kmol) and large diffusion coefficient ($D_{AB} \approx 1.009 \times 10^{-9}$ m^2/s; Table 1; Wilke & Chang, 1955), and we confirmed diffusion by [^{14}C]-labeled glucose transport assay (Figure 3). To further enhance glucose uptake, SCVE was co-expressed in the *E. coli* outer membrane (Figure 2a), which can permeabilize outer membranes of *E. coli* cells by forming transmembrane pores (Liao, Lescar, Tam, & Liu, 2004). This reduced permeation barrier of the outer membrane might increase the glucose concentration in the periplasm, thus increasing the glucose gradient across the SecY (ΔP) channel, accelerating glucose diffusion into the cytoplasm (Figure 3), and increasing *E. coli* (ΔPtsG) growth on glucose (Figure 2b). The glucose PTS catalyzes transport with concomitant phosphorylation of glucose to glucose-6-phosphate. Therefore, once glucose is inside the mutant *E. coli* cells, phosphorylation might become the factor limiting glycolytic flux (Hernández-Montalvo et al., 2003), explaining the full recovery of *E. coli* (ΔPtsG) growth on glucose with overexpression of an *E. coli* glucokinase (Glk; Fukuda, Yamaguchi, Shimosaka, Murata, & Kimura, 1983) together with SecY (ΔP) and SCVE (Figure 2b). We compared the Monod growth kinetic parameters of *E. coli* (ΔPtsG) co-expressing SecY (ΔP), SCVE, and Glk with those of the wild-type strain (Figure 2c). Both strains had a maximum specific growth rate (μ_{max}) of 0.347 hr^{-1}, but the half-saturation constant (K_S) of the mutant strain (≈ 4.803 mM) was 0.49-fold higher than that of the wild-type *E. coli* (≈ 3.234 mM), indicating

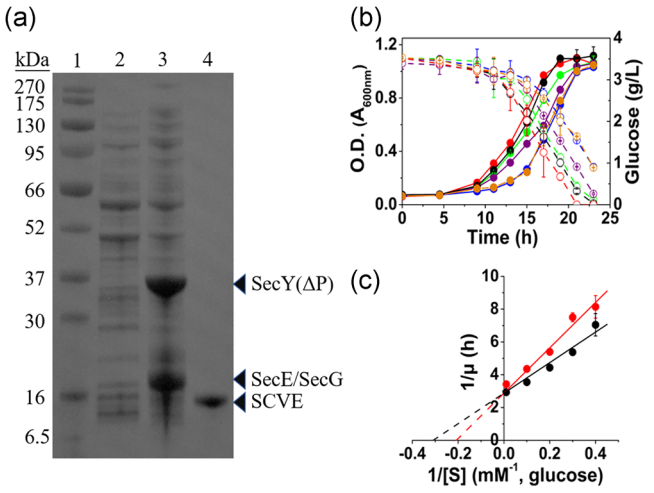

FIGURE 2 Uptake of glucose via SecY (ΔP). (a) SDS-PAGE analysis. Marker (lane 1), *Escherichia coli* (ΔPtsG) containing pETDuet-1 and pRSFDuet-1 (lane 2), *E. coli* (ΔPtsG) containing pETDuet-*secY (ΔP)-secE* and pRSFDuet-*secG* (lane 3), the His-tagged SCVE from *E. coli* (ΔPtsG) containing *pETDuet-secY (ΔP)-secE* and pRSFDuet-*secG-sCVE·His* (lane 4). (b,c) Growth of *E. coli* in M9 medium with glucose. Wild-type *E. coli* (black), *E. coli* (ΔPtsG) (blue), *E. coli* (ΔPtsG) with SecY (ΔP) (purple), *E. coli* (ΔPtsG) with SCVE (orange), *E. coli* (ΔPtsG) with SecY (ΔP) and SCVE (green), *E. coli* (ΔPtsG) with SecY (ΔP), SCVE and Glk (red). Error bars, *SD*, *n* = 3. Glk, glucokinase; SCVE, SARS coronavirus envelope protein; SDS-PAGE, sodium dodecyl sulfate polyacrylamide gel electrophoresis [Color figure can be viewed at wileyonlinelibrary.com]

TABLE 1 The molal volume (V_A) and diffusion coefficient (D_{AB}) in water at 37°C

Solute A	Glucose	Fructose	Mannose	Xylose	Arabinose	Lactose	2-NBDG
Molecular formula	$C_6H_{12}O_6$			$C_5H_{10}O_5$		$C_{12}H_{22}O_{11}$	$C_{12}H_{14}N_4O_8$
V_A (m^3/kmol)	0.178			0.148		0.340	0.347
D_{AB} (m^2/s)	1.009×10^{-9}			1.127×10^{-9}		0.684×10^{-9}	0.676×10^{-9}

that the SecY (ΔP) channel had a lower affinity for glucose than the glucose PTS.

Then, we selected fructose and mannose as two other PTS-dependent hexoses for examination. *E. coli* with damaged fructose PTS (ΔFruA; Ferenci & Kornberg, 1974) or mannose PTS (ΔManXYZ; Erni & Zanolari, 1985) did not grow on fructose (Figure 4a) or mannose (Figure 4c), respectively. In contrast, SecY (ΔP) and SCVE were found to help both mutant strains, especially those on mannose, recover growth. Co-expression of an *E. coli* fructo(manno)kinase (Mak) that catalyzes phosphorylation of fructose or mannose in the cytoplasm (Sproul, Lambourne, Jean-Jacques, & Kornberg, 2001) allowed the FruA-lacking strain to grow on fructose at a similar rate as that of wild-type *E. coli* (Figure 4a). Growth of the strain without ManXYZ on mannose was even faster than that of the control (Figure 4c), suggesting that fructose or mannose imported by the SecY (ΔP) channel satisfied demands of the cells. Here, it should be noted that fructose taken up via the fructose PTS is phosphorylated to fructose-1-phosphate before phosphorylation to fructose-1,6-bisphosphate (Kornberg, 2001). However, in the route established in this study, the phosphorylated fructose first appeared inside the cell as fructose-6-phosphate (Figure 1b), which accords with use of the PtsG-F transporter (Kornberg, Lambourne, & Sproul, 2000). The growth kinetics in Figure 4b,d show that co-expression of SecY (ΔP), SCVE, and Mak conferred almost the same μ_{max} values (0.248 hr^{-1} on fructose and 0.398 hr^{-1} on mannose) on the mutant *E. coli* as those of the wild-type strain. Also, as in the case of glucose, the SecY (ΔP) channel exhibited a lower affinity for fructose ($K_S \approx 1.579$ mM) and mannose ($K_S \approx 4.719$ mM) than for the fructose PTS ($K_S \approx 0.843$ mM) and mannose PTS ($K_S \approx 3.181$ mM).

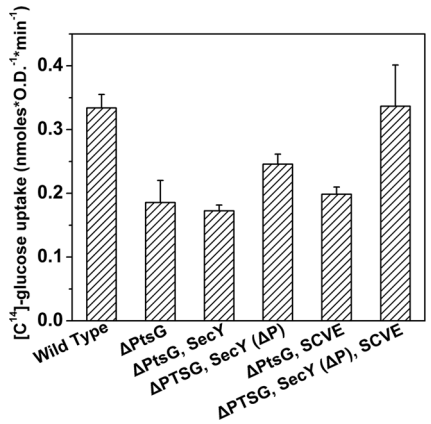

FIGURE 3 Uptake of [C^{14}]-glucose by various *Escherichia coli* strains. SecY indicates cells overexpressing the wild-type SecY channel. Error bars, *SD*, $n = 3$. SCVE, SARS coronavirus envelope protein

3.2 | Functional transport of the non-PTS-dependent pentoses via the SecY (ΔP) channel

Next, we tested xylose and arabinose, which are non-PTS-dependent pentoses. The main transporters for xylose (XylFGH; Sumiya, Davis, Packman, McDonald, & Henderson, 1995) and arabinose (AraFGH, AraE; Schleif, 2000) in *E. coli* were deleted independently; thus, the obtained strains either did not grow on xylose (Figure 5a) or arabinose (Figure 5c) as the sole carbon source. As expected, co-expression of SecY (ΔP) and SCVE fully supported the growth of mutants. The lag phases of both mutant strains were shortened when compared with wild-type *E. coli*, as was the case with mannose (Figure 4c). Interestingly, previous work showed that a mutant glucose facilitator protein (2-RD5) from *Zymomonas mobilis* in *E. coli* allowed rapid transport of xylose

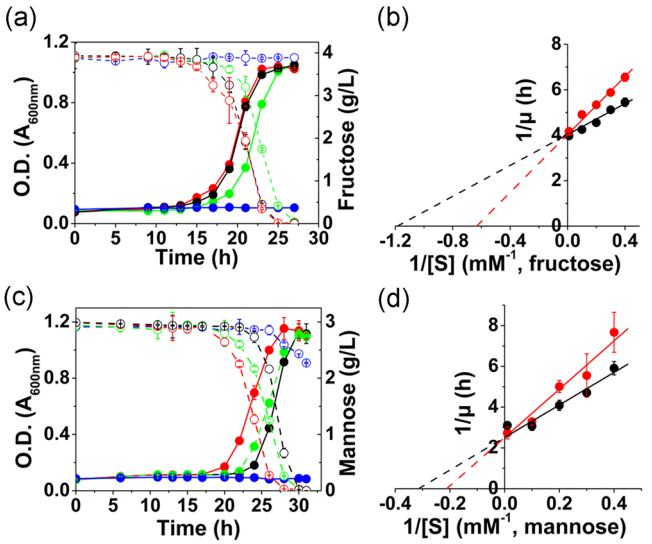

FIGURE 4 Uptake of fructose and mannose via SecY (ΔP). (a,b) Growth of *Escherichia coli* in M9 medium with fructose. Wild-type *E. coli* (black), *E. coli* (ΔFruA) (blue), *E. coli* (ΔFruA) with SecY (ΔP) and SCVE (green), *E. coli* (ΔFruA) with SecY (ΔP), SCVE and Mak (red). (c,d) Growth of *E. coli* in M9 medium with mannose. Wild-type *E. coli* (black), *E. coli* (ΔManXYZ) (blue), *E. coli* (ΔManXYZ) with SecY (ΔP) and SCVE (green), *E. coli* (ΔManXYZ) with SecY (ΔP), SCVE and Mak (red). Error bars, *SD*, $n = 3$. SCVE, SARS coronavirus envelope protein [Color figure can be viewed at wileyonlinelibrary.com]

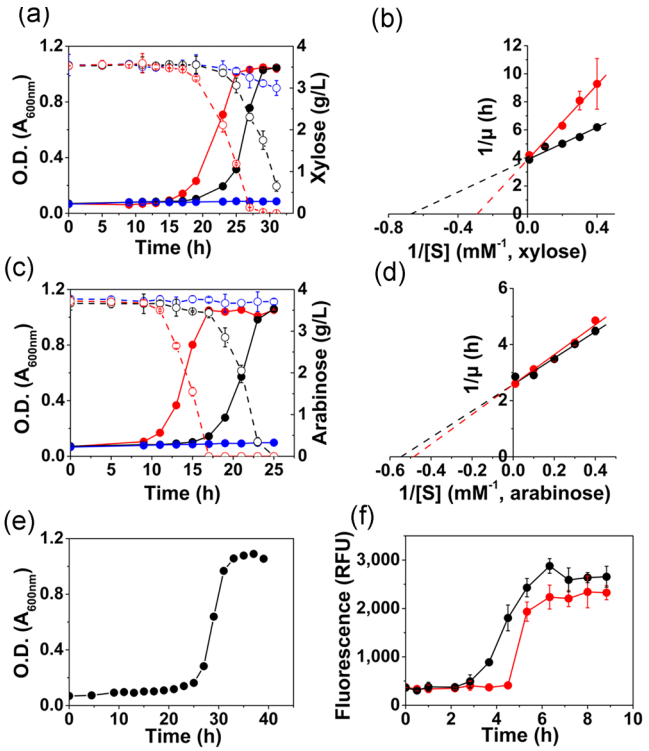

FIGURE 5 Uptake of xylose and arabinose via SecY (ΔP). (a,b) Growth of *Escherichia coli* in M9 medium with xylose. Wild-type *E. coli* (black), *E. coli* (ΔXylFGH) (blue), *E. coli* (ΔXylFGH) with SecY (ΔP) and SCVE (red). (c,d) Growth of *E. coli* in M9 medium with arabinose. Wild-type *E. coli* (black), *E. coli* (ΔAraFGH, ΔAraE) (blue), *E. coli* (ΔAraFGH, ΔAraE) with SecY (ΔP) and SCVE (red). (e) Growth of *E. coli* (ΔAraFGH, ΔAraE) re-expressing AraFGH with SCVE in M9 medium containing 4 g/L of arabinose. The *araFGH* genes were expressed with *sCVE* via plasmids in *E. coli* BL21 (DE3) with genomic *araFGH* and *araE* deleted. (f) Expression kinetics of GFP under control of the promoter P_{BAD}. Wild-type *E. coli* (red), *E. coli* (ΔAraFGH, ΔAraE) with SecY (ΔP) and SCVE (black). Error bars, *SD*, $n = 3$. GFP, green fluorescent protein; SCVE, SARS coronavirus envelope protein [Color figure can be viewed at wileyonlinelibrary.com]

but also caused an extensive growth delay (Ren, Chen, Zhang, Liang, & Lin, 2009). A prolonged lag phase (≈ 25 hr) on arabinose was also observed when we re-expressed AraFGH together with SCVE in *E. coli* (ΔAraFGH, ΔAraE; Figure 5e), even though AraFGH is regarded as an efficient system for arabinose uptake (Luo et al., 2014). Use of the SecY (ΔP) channel did not seem to facilitate the initiation of the arabinose-inducible promoter P_{BAD} (Desai & Rao, 2010; Figure 5f), which controls synthesis of key enzymes (AraBAD) in the arabinose metabolism pathway in *E. coli* (Schleif, 2000). Therefore, we suspect that the SecY (ΔP) channel transports other small nutritional molecules, allowing the cells to adapt to the growth conditions more quickly than the wild-type strain at the beginning of fermentation. The mutant strain expressing SecY (ΔP) with SCVE showed a μ_{max} of 0.258 hr^{-1} on xylose (Figure 5b) and 0.388 hr^{-1} on arabinose (Figure 5d), which were almost identical to those of the wild-type *E. coli*. The K_S values for the mutant strains were 3.449 and 2.066 mM on xylose and arabinose, respectively, whereas, for wild-type *E. coli*, the values were 1.489 and 1.831 mM.

3.3 | Functional transport of disaccharide via the SecY (ΔP, IIIGIG) channel

Next, we investigated the transport of lactose as a model disaccharide via the SecY (ΔP) channel. The LacY transporter (Abramson et al., 2003) was deleted from *E. coli* and thus the mutant strain could not grow on lactose as the sole carbon source (Figure 6a). However, the growth of *E. coli* (ΔLacY) was slow after co-expression of SecY (ΔP) and SCVE, probably because the larger molecular volume of lactose ($V_A \approx 0.340\ m^3/kmol$) led to a lower diffusion coefficient ($D_{AB} \approx 0.684 \times 10^{-9}\ m^2/s$) than the coefficient for monosaccharides ($V_A \leq 0.178\ m^3/kmol$, $D_{AB} \geq 1.009 \times 10^{-9}\ m^2/s$) (Table 1), resulting in reduced sugar flux through the pore ring of SecY (ΔP). We then replaced the isoleucines (molecular weight $Mr \approx 131.18$ g/mol) in the pore ring with glycines ($Mr \approx 75.07$ g/mol) to enlarge the channel opening (Figure 6b). As illustrated in Figure 6c, glycine substitutions at Ile 191 and Ile 408 (SecY (ΔP, IIIGIG)) provoked a 1.27-fold increase in permeation rate of 2-NBDG, which has almost the same V_A and D_{AB} as those of lactose (Table 1). With co-expression of SecY (ΔP, IIIGIG) and SCVE, *E. coli* (ΔLacY) exhibited moderate growth on lactose, 50 hr after

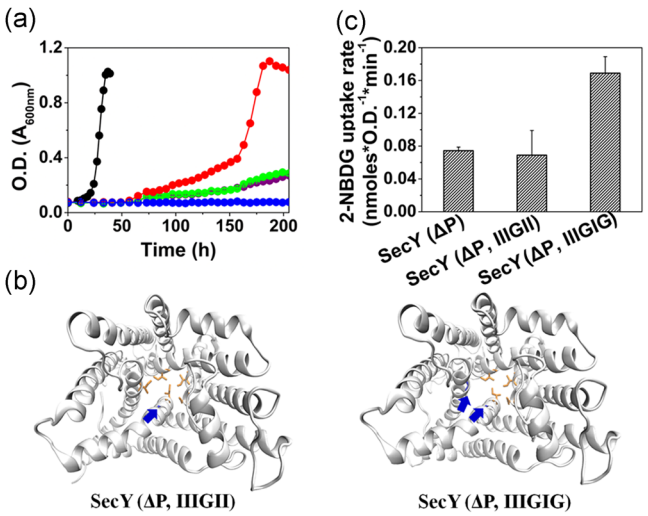

FIGURE 6 Uptake of lactose via SecY (ΔP, IIIGIG). (a) Growth of *Escherichia coli* in M9 medium with 4 g/L of lactose. Wild-type *E. coli* (black), *E. coli* (ΔLacY) (blue), *E. coli* (ΔLacY) with SecY (ΔP) and SCVE (purple), *E. coli* (ΔLacY) with SecY (ΔP, IIIGII) and SCVE (green), *E. coli* (ΔLacY) with SecY (ΔP, IIIGIG) and SCVE (red). (b) Bottom view of three-dimensional SecY (ΔP, IIIGII) and SecY (ΔP, IIIGIG) structures, with PDBID 3J46 used as a template in homology modeling (Modeller v9.18). Pore-ring residues of SecY (ΔP, IIIGII): Ile 82, Ile 86, Ile 187, Gly 191, Ile 278, Ile 408. Pore-ring residues of SecY (ΔP, IIIGIG): Ile 82, Ile 86, Ile 187, Gly 191, Ile 278, Gly 408. (c) Rates of 2-NBDG transport through SecY mutants in *E. coli* (ΔPtsG) with SCVE. Error bars, *SD*, $n = 3$. 2-NBDG, 2-deoxy-2-[(7-nitro-2,1,3-benzoxadiazol-4-yl)amino]-D-glucose; SCVE, SARS coronavirus envelope protein [Color figure can be viewed at wileyonlinelibrary.com]

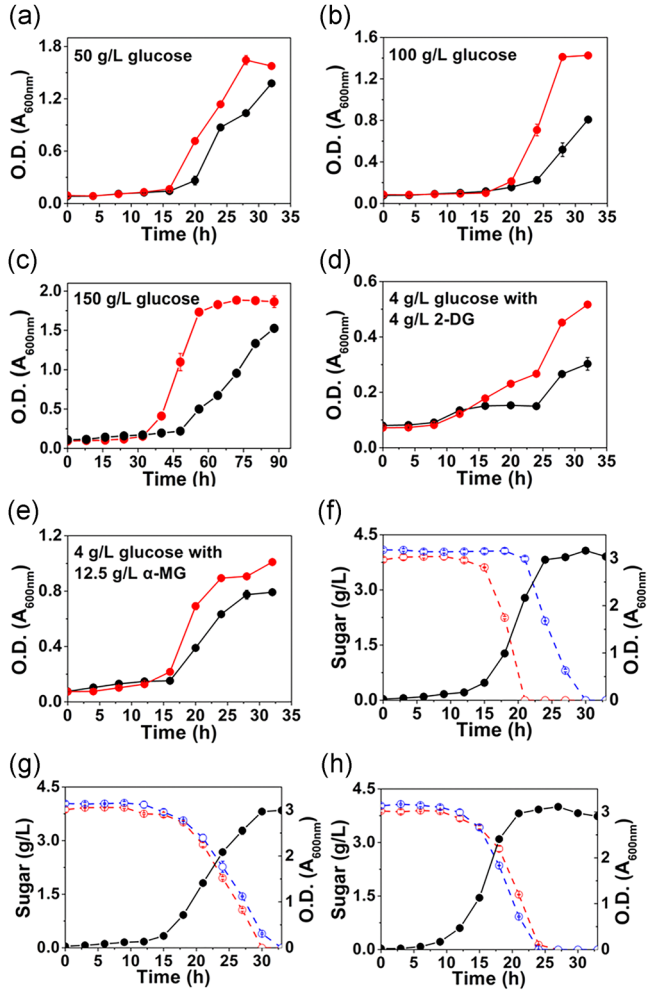

FIGURE 7 Benefits of using SecY(ΔP) for sugar uptake. In (a–e), M9 medium, wild-type *Escherichia coli* (black), *E. coli* (ΔPtsG) with SecY (ΔP), SCVE and Glk (red). In (f–h), M9 medium, cell density (black), glucose (red), and xylose (blue). Strains: (f) wild-type *E. coli*; (g) *E. coli* (ΔPtsG); (h) *E. coli* (ΔPtsG) with SecY (ΔP), SCVE, and Glk. Error bars, *SD*, $n = 3$. Glk, glucokinase; SCVE, SARS coronavirus envelope protein [Color figure can be viewed at wileyonlinelibrary.com]

cell inoculation (Figure 6a). It is interesting that the SecY (ΔP, IIIGIG)-engineered *E. coli* (ΔLacY) was able to grow with a rate almost similar to the wild-type after 160 hr. The possible reason is that wild-type *E. coli* may have other unknown systems that can transport lactose in addition to LacY, but these systems have extremely low expression levels when the wild-type *E. coli* grows on lactose. In this case, the engineered channel allows moderate growth of *E. coli* (ΔLacY), offering a prerequisite for adaption. After a long-term cultivation, other endogenous transport systems for lactose may be activated.

3.4 | Benefits of using the mutant SecY channel for sugar transport

Sugar passage via specific transporters exhibits nonlinear kinetics as the external sugar content increases, demonstrating transport saturation (Cirillo, 1961). Large sugar gradients across a cell membrane can even inhibit growth. As shown in Figure 7a–c, the specific growth rates of *E. coli* at 50, 100, and 150 g/L of glucose were 0.137, 0.127, and 0.036 hr^{-1}, whereas the rates of *E. coli* (ΔPtsG) with SecY (ΔP), SCVE, and Glk were 0.175, 0.228, and 0.103 hr^{-1}, respectively. This indicates that the use of SecY (ΔP) channel can probably reduce the effects of transport saturation and increase the tolerance of *E. coli* for glucose, thereby improving cell growth at high sugar levels. Moreover, Figure 7d and e suggest that the modified SecY (ΔP) channel reduced competitive inhibition of glucose transport in *E. coli* by glucose analogs methyl-α-D-glucoside (α-MG) and 2-deoxy-D-glucose (2-DG). When simultaneous utilization of mixed monosaccharides by the channel-engineered *E. coli* was tested, we found that wild-type *E. coli* exhibited CCR when grown in the presence of glucose and xylose, as expected (Figure 7f). Previous efforts have revealed that the PTS for the preferred carbon source plays a major role in CCR regulation (Deutscher, Francke, & Postma, 2006; Gorke & Stülke, 2008). However, deletion of the glucose PTS can lead to reduced glucose uptake (Kim et al., 2015; Figure 7g). Our results show that replacing the glucose PTS with SecY (ΔP), SCVE, and Glk enabled *E. coli* cells to simultaneously utilize glucose and xylose (Figure 7h) to overcome CCR. In addition, the consumption of both sugars accelerated compared with that of non-channel-engineered *E. coli* (ΔPtsG), with a specific growth rate that increased from 0.174 to 0.309 hr^{-1}.

ACKNOWLEDGMENTS

We are grateful to Dr. Jun-Cheng Liang and Xiang-Ping Qiu (National Institute of Metrology) for radioisotope analysis. This study was supported by the National Key Research and Development of China (no. 2016YFA0204300), National Natural Science Foundation of China (no. 21776010 and 21978014), and International Clean Energy Talent Program of China Scholarship Council (no. 201802180008).

ORCID

Qiang Guo http://orcid.org/0000-0001-7148-9163

REFERENCES

Abramson, J., Smirnova, I., Kasho, V., Verner, G., Kaback, H. R., & Iwata, S. (2003). Structure and mechanism of the lactose permease of *Escherichia coli*. *Science*, *301*(5633), 610–615. https://doi.org/10.1126/science.1088196

Akimaru, J., Matsuyama, S., Tokuda, H., & Mizushima, S. (1991). Reconstitution of a protein translocation system containing purified SecY, SecE, and SecA from *Escherichia coli*. *Proceedings of the National Academy of Sciences*, *88*(15), 6545–6549. https://doi.org/10.1073/pnas.88.15.6545

Breyton, C., Haase, W., Rapoport, T. A., Kühlbrandt, W., & Collinson, I. (2002). Three-dimensional structure of the bacterial protein-translocation complex SecYEG. *Nature*, *418*(6898), 662–665. https://doi.org/10.1038/nature00827

Brundage, L., Hendrick, J. P., Schiebel, E., Driessen, A. J. M., & Wickner, W. (1990). The purified *E. coli* integral membrane protein SecYE is sufficient for reconstitution of SecA-dependent precursor protein translocation. *Cell*, *62*(4), 649–657. https://doi.org/10.1016/0092-8674(90)90111-q

Chen, L. Q., Cheung, L. S., Feng, L., Tanner, W., & Frommer, W. B. (2015). Transport of sugars. *Annual Review of Biochemistry*, *84*, 865–894. https://doi.org/10.1146/annurev-biochem-060614-033904

Chen, P. T., Chiang, C. J., Wang, J. Y., Lee, M. Z., & Chao, Y. P. (2011). Genomic engineering of *Escherichia coli* for production of intermediate metabolites in the aromatic pathway. *Journal of the Taiwan Institute of Chemical Engineers*, *42*(1), 34–40. https://doi.org/10.1016/j.jtice.2010.03.010

Cirillo, V. P. (1961). Sugar transport in microorganisms. *Annual Review of Microbiology*, *15*(1), 197–218. https://doi.org/10.1146/annurev.mi.15.100161.001213

Datsenko, K. A., & Wanner, B. L. (2000). One-step inactivation of chromosomal genes in *Escherichia coli* K-12 using PCR products. *Proceedings of the National Academy of Sciences*, *97*(12), 6640–6645. https://doi.org/10.1073/pnas.120163297

Desai, T. A., & Rao, C. V. (2010). Regulation of arabinose and xylose metabolism in *Escherichia coli*. *Applied and Environmental Microbiology*, *76*(5), 1524–1532. https://doi.org/10.1128/AEM.01970-09

Deutscher, J., Francke, C., & Postma, P. W. (2006). How phosphotransferase system-related protein phosphorylation regulates carbohydrate metabolism in bacteria. *Microbiology and Molecular Biology Reviews*, *70*(4), 939–1031. https://doi.org/10.1128/MMBR.00024-06

Erni, B., & Zanolari, B. (1985). The mannose-permease of the bacterial phosphotransferase system. Gene cloning and purification of the enzyme IIManIIIMan complex of *Escherichia coli*. *The Journal of Biological Chemistry*, *260*(29), 15495–15503.

Ferenci, T., & Kornberg, H. L. (1974). The role of phosphotransferase-mediated syntheses of fructose 1-phosphate and fructose 6-phosphate in the growth of *Escherichia coli* on fructose. *Proceedings of the Royal Society of London. Series B: Biological Sciences*, *187*(1087), 105–119. https://doi.org/10.1098/rspb.1974.0065

Fukuda, Y., Yamaguchi, S., Shimosaka, M., Murata, K., & Kimura, A. (1983). Cloning of the glucokinase gene in *Escherichia coli* B. *Journal of Bacteriology*, *156*(2), 922–925.

Gorke, B., & Stülke, J. (2008). Carbon catabolite repression in bacteria: Many ways to make the most out of nutrients. *Nature Reviews Microbiology*, *6*(8), 613–624. https://doi.org/10.1038/nrmicro1932

Hernández-Montalvo, V., Martínez, A., Hernández-Chavez, G., Bolivar, F., Valle, F., & Gosset, G. (2003). Expression of galP and glk in a *Escherichia coli* PTS mutant restores glucose transport and increases glycolytic flux to fermentation products. *Biotechnology and Bioengineering*, *83*(6), 687–694. https://doi.org/10.1002/bit.10702

Joung, S. M., Kurumbang, N. P., Sang, B. I., & Oh, M. K. (2011). Effects of carbon source and metabolic engineering on butyrate production in *Escherichia coli*. *Korean Journal of Chemical Engineering*, *28*(7), 1587–1592. https://doi.org/10.1007/s11814-011-0032-6

Kim, S. M., Choi, B. Y., Ryu, Y. S., Jung, S. H., Park, J. M., Kim, G. H., & Lee, S. K. (2015). Simultaneous utilization of glucose and xylose via novel mechanisms in engineered *Escherichia coli*. *Metabolic Engineering*, *30*, 141–148. https://doi.org/10.1016/j.ymben.2015.05.002

Kornberg, H. L. (2001). Routes for fructose utilization by *Escherichia coli*. *Journal of Molecular Microbiology and Biotechnology*, *3*(3), 355–359.

Kornberg, H. L., Lambourne, L. T. M., & Sproul, A. A. (2000). Facilitated diffusion of fructose via the phosphoenolpyruvateglucose phosphotransferase system of *Escherichia coli*. *Proceedings of the National Academy of Sciences*, *97*(4), 1808–1812. https://doi.org/10.1073/pnas.97.4.1808

Li, L., Park, E., Ling, J., Ingram, J., Ploegh, H., & Rapoport, T. A. (2016). Crystal structure of a substrate-engaged SecY protein-translocation channel. *Nature*, *531*(7594), 395–399. https://doi.org/10.1038/nature17163

Li, W., Schulman, S., Boyd, D., Erlandson, K., Beckwith, J., & Rapoport, T. A. (2007). The plug domain of the SecY protein stabilizes the closed state of the translocation channel and maintains a membrane seal. *Molecular Cell*, *26*(4), 511–521. https://doi.org/10.1016/j.molcel.2007.05.002

Liao, Y., Lescar, J., Tam, J. P., & Liu, D. X. (2004). Expression of SARS-coronavirus envelope protein in *Escherichia coli* cells alters membrane permeability. *Biochemical and Biophysical Research Communications*, *325*(1), 374–380. https://doi.org/10.1016/j.bbrc.2004.10.050

Luo, Y., Zhang, T., & Wu, H. (2014). The transport and mediation mechanisms of the common sugars in *Escherichia coli*. *Biotechnology Advances*, *32*(5), 905–919. https://doi.org/10.1016/j.biotechadv.2014.04.009

Mandon, E. C., Trueman, S. F., & Gilmore, R. (2009). Translocation of proteins through the Sec61 and SecYEG channels. *Current Opinion in Cell Biology*, *21*(4), 501–507. https://doi.org/10.1016/j.ceb.2009.04.010

Osborne, A. R., Rapoport, T. A., & Van den Berg, B. (2005). Protein translocation by the Sec61/SecY channel. *Annual Review of Cell and Developmental Biology*, *21*(1), 529–550. https://doi.org/10.1146/annurev.cellbio.21.012704.133214

Park, E., & Rapoport, T. A. (2011). Preserving the membrane barrier for small molecules during bacterial protein translocation. *Nature*, *473*(7346), 239–242. https://doi.org/10.1038/nature10014

Pontrelli, S., Chiu, T. Y., Lan, E. I., Chen, F. Y., Chang, P., & Liao, J. C. (2018). *Escherichia coli* as a host for metabolic engineering. *Metabolic Engineering*, *50*, 16–46. https://doi.org/10.1016/j.ymben.2018.04.008

Rapoport, T. A. (2007). Protein translocation across the eukaryotic endoplasmic reticulum and bacterial plasma membranes. *Nature*, *450*(7170), 663–669. https://doi.org/10.1038/nature06384

Reinhold, L., & Kaplan, A. (1984). Membrane transport of sugars and amino acids. *Annual Review of Plant Physiology*, *35*(1), 45–83. https://doi.org/10.1146/annurev.pp.35.060184.000401

Ren, C., Chen, T., Zhang, J., Liang, L., & Lin, Z. (2009). An evolved xylose transporter from *Zymomonas mobilis* enhances sugar transport in *Escherichia coli*. *Microbial Cell Factories*, *8*(1), 66. https://doi.org/10.1186/1475-2859-8-66

Schleif, R. (2000). Regulation of the L-arabinose operon of *Escherichia coli*. *Trends in Genetics*, *16*(12), 559–565. https://doi.org/10.1016/s0168-9525(00)02153-3

Sproul, A. A., Lambourne, L. T. M., Jean-Jacques, D. J., & Kornberg, H. L. (2001). Genetic control of manno(fructo)kinase activity in *Escherichia coli*. *Proceedings of the National Academy of Sciences*, *98*(26), 15257–15259. https://doi.org/10.1073/pnas.211569798

Stülke, J., & Hillen, W. (1999). Carbon catabolite repression in bacteria. *Current Opinion in Microbiology*, *2*(2), 195–201. https://doi.org/10.1016/s1369-5274(99)80034-4

Sumiya, M., Davis, E. O., Packman, L. C., McDonald, T. P., & Henderson, P. J. (1995). Molecular genetics of a receptor protein for D-xylose, encoded by the gene xylF, in *Escherichia coli*. *Receptors & Channels*, *3*(2), 117–128.

Tam, P. C., Maillard, A. P., Chan, K. K., & Duong, F. (2005). Investigating the SecY plug movement at the SecYEG translocation channel. *The EMBO Journal*, *24*(19), 3380–3388. https://doi.org/10.1038/sj.emboj.7600804

Van den Berg, B., Clemons, W. M., Collinson, I., Modis, Y., Hartmann, E., Harrison, S. C., & Rapoport, T. A. (2004). X-ray structure of a protein-conducting channel. *Nature*, *427*(6969), 36–44. https://doi.org/10.1038/nature02218

Wilke, C. R., & Chang, P. (1955). Correlation of diffusion coefficients in dilute solutions. *AIChE Journal*, *1*(2), 264–270. https://doi.org/10.1002/aic.690010222

Yoshioka, K., Takahashi, H., Homma, T., Saito, M., Oh, K. B., Nemoto, Y., & Matsuoka, H. (1996). A novel fluorescent derivative of glucose applicable to the assessment of glucose uptake activity of *Escherichia coli*. *Biochimica et Biophysica Acta—General Subjects*, *1289*(1), 5–9. https://doi.org/10.1016/0304-4165(95)00153-0

Zhao, F., Zhao, Y., Liu, Y., Chang, X., Chen, C., & Zhao, Y. (2011). Cellular uptake, intracellular trafficking, and cytotoxicity of nanomaterials. *Small*, *7*(10), 1322–1337. https://doi.org/10.1002/smll.201100001

SUPPORTING INFORMATION

Additional supporting information may be found online in the Supporting Information section.

How to cite this article: Guo Q, Mei S, Xie C, et al. Reprogramming of sugar transport pathways in *Escherichia coli* using a permeabilized SecY protein-translocation channel. *Biotechnology and Bioengineering*. 2020;117:1738–1746. https://doi.org/10.1002/bit.27306